0273-2289/98/70–72—0463$12.00

Adaptive Optimal Control of Fed-Batch Alcoholic Fermentation

T. L. M. Alves,* A. C. Costa, A. W. S. Henriques, and E. L. Lima

PEQ/COPPE/UFRJ, Cx. Postal 68502, CEP 21945–970, Rio de Janeiro, RJ, Brazil

ABSTRACT

An adaptive control scheme is developed for the optimization of a fed-batch ethanol production process. The fermentation process is modeled by an hybrid neural model combining mass balance equations and neural networks, used to represent the kinetic rates. The networks used, the functional link networks (FLN), allow the linear estimation of their parameters; this enables the re-estimation of the parameters at each sampling time, and thus the development of an adaptive optimal control scheme.

Index Entries: Ethanol production; optimal control; hybrid neural modeling; adaptive control.

INTRODUCTION

Brazil is the main ethanol producer in the world. This position is the result of a political strategy initiated in 1975 by the Brazilian government to cope with the sharp increase in petroleum oil prices at that time. The objective of the Brazilian National Program (PROALCOOL) was to encourage the traditional alcohol industries to increase their ethanol production in order to replace gasoline with ethanol as a main automobile fuel. Because the main objective was production, and not necessarily efficiency, a significant sector of this industry, mainly those companies with a family-based structure, have not been investing in technology. Currently, because of the stabilization of the petroleum prices at a low level and the necessity of increasing the efficiency of public administration, the government has withdrawn most of the incentives to the alcohol industry. With this new reality, only those industries that are technically efficient will continue in

* Author to whom all correspondence and reprint requests should be addressed.

the market. Therefore, there is an increased interest in optimizing all the steps of the ethanol production process.

In the optimization of fed-batch processes, the objective is to determine the substrate addition strategy that maximizes the product of interest at the end of the batch cycle. This is an optimal control problem and there are various methods proposed for its solution. Palanki et al. *(1)* used Pontryagin's maximum principle and the singular control theory. Cuthrell and Biegler *(2)* proposed a simultaneous optimization and solution strategy based on successive quadratic programming (SQP) and orthogonal collocation on finite elements. Luus *(3)* utilized iterative dynamic programming to provide piecewise linear continuous control policies. Costa (4) proposed a methodology to obtain optimal trajectories analytically and in feedback mode.

Once the optimization problem is solved off-line, the calculated profile of the control variable can be implemented in an open-loop fashion. This approach is appropriate in situations in which process model is accurately known and there are no external disturbances to the process.

Because fed-batch processes are transient in nature and their variables undergo significant changes during the fermentation, it is desirable that the precalculated trajectories be corrected on-line. To this end, several authors have studied different approachs. Terwiesch and Agarwal *(5)* developed a method for on-line correction of preoptimized input profiles. Lee and Ramirez *(6)* used an extended Kalman filter to estimate state variables and parameters, and implemented an on-line optimal control scheme in a process for induced foreign protein production.

However, in most real-time applications, the on-line correction of preoptimized profiles is infeasible because of prohibitive computing-power requirements *(5)*. The great difficulty is usually associated with the on-line estimation of the kinetic parameters, because they lead to the nonlinearity of the model equations.

In this work, an hybrid neural model of the process is developed. This model combines *a priori* knowledge of the process and neural networks, which are used for the estimation of the kinetic rates. Psichogios and Ungar *(7)* were the first to investigate the application of this modeling procedure to a fed-batch bioreactor. More recently, Schubert et al. *(8)* applied an improved technique of hybrid modeling to a fed-batch baker's yeast production process, and Fu and Barford *(9)* developed a hybrid neural model for a complex simulation of hybridoma cell cultivation for monoclonal antibody (Mab) production.

The goal of the hybrid neural modeling in this case is to deal with the problem of the on-line estimation. Thus, the kind of neural networks chosen to describe the kinetic rates are the functional link networks (FLN), whose great advantage is that the estimation of the network parameters is linear and it ensures convergence *(10)*. Besides, a modification is applied to these networks to increase the nonlinear approximation ability *(11)*.

A method based on orthogonal least-squares is used to eliminate non-significant nodes during the training of the network. This method was originally used for the identification of a multivariable non-linear systems by Billings et al. *(12)*. The use of this method significantly reduces the size and complexity of the network, and avoids overfitting of the data.

The hybrid neural model allied to the structure chosen for the neural networks make the on-line estimation of the kinetic rates very easy, and enables the development of an adaptive optimal control scheme in which the trajectory of the control variable calculated off-line is corrected at each sampling time.

The ethanol production via fementation in a fed-batch bioreactor is a typical example of a process in which the proposed strategy could be beneficial. The microorganism most used in this process is *Sacharomyces cerevisae*. However, ethanol production by *Zymomonas mobilis* can be considered a good alternative, because of its advantages when compared to *S. cerevisae*, including higher ethanol yield (to 97% of theoretical value), higher ethanol productivity, and better tolerance to acid and high concentrations of sugar and alcohol *(13)*.

This research is part of an effort to develop a new technology for ethanol production by *Z. mobilis*. At a first stage, the algorithm is tested on the best-known *S. cerevisae* process. However, a more complex process will not modify the main results, but only require more involved details.

METHODS

Hybrid Neural Model

The hybrid neural model is a combination of the mass balance equations and neural networks, used to calculate the kinetic rates.

Mass Balance Equations

The mass balance equations for a fed-batch ethanol fermentation are

$$dX/dt = (\mu - D)X \tag{1}$$

$$dS/dt = -\sigma X + D(S_F - S) \tag{2}$$

$$dP/dt = \pi X - DP \tag{3}$$

$$dV/dt = DV \tag{4}$$

where X, S, and P are the biomass, substrate, and ethanol concentrations; μ, σ, and π are the specific rates of growth, substrate consumption, and ethanol formation, respectively; S_F is the feed substrate concentration, D is the dilution rate, defined as $D = F/V$; F is the volumetric substrate feed rate, V is the volume of the reactor mixture, and t is the elapsed time.

Functional Link Networks

A neural network typically consists of many simple computational elements or nodes arranged in layers and operating in parallel. The weights, which define the strength of connection between the nodes, are estimated to yield good performance. Usually, in the training of neural networks, the inputs to a node are linearly weighted before the sum is passed through some nonlinear activation function that ultimately gives the network its nonlinear approximation ability. The same nonlinearity, however, creates problems in learning the network weights, because nonlinear learning rules must be used. The learning rate is often unacceptably slow and local minima may cause problems *(10)*.

One way of avoiding nonlinear learning is the use of FLNs. In these networks, a nonlinear functional transform or expansion of the network inputs is initially performed, and then the resulting terms are combined linearly. The resulting structure has a good nonlinear approximation capability, and the estimation of the network weights is linear.

The general structure of a FLN is shown in Fig. 1, where x_e is the input vector and $y_i(x_e)$ is an output. The hidden layer performs a functional expansion on the inputs, in terms of nonlinear functions $h_j(x_e)$, which maps the input space, of dimension n_1, onto a new space of increased dimension, M ($M > n_1$). The output layer consists of m nodes, and each node is, in fact, a linear combiner. The input–output relationship of the FLN is

$$y_i(x_e) = \sum_{j=1}^{M} w_{ij}h_j(x_e), \qquad 1 \le i \le m \tag{5}$$

Henrique *(11)* proposed a modification in the structure of the FLNs, in which the output given by Eq. 5 is passed through an invertible nonlinear activation function. The new output is

$$y_i(x_e) = f_i\left(\sum_{j=1}^{M} w_{ij}h_j(x_e)\right), \qquad 1 \le i \le m \tag{6}$$

where f_i is an invertible nonlinear function, as for example:

$$f_i(y_i) = \tanh(y_i) = \left(1 - \exp(-2y_i)\right)\Big/\left(1 + \exp(-2y_i)\right) \tag{7}$$

The proposed modification increases the nonlinear approximation ability of the network, and yet the estimation of the parameters remains a linear problem.

The network inputs(xe), in this case, are the biomass, substrate, and ethanol concentrations, which are supposed to be known in different sampling times. The network output (y), is the kinetic rate to be calculated. In order to obtain output values for the network training, a discrete model can be obtained from Eqs. 1–3:

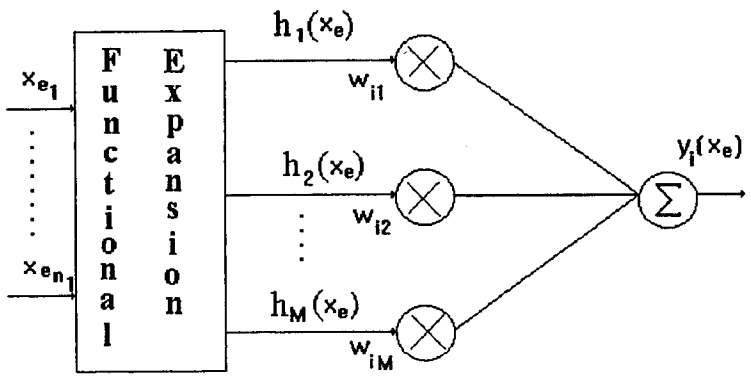

Fig. 1. General structure of a FLN.

$$\mu(t) = \left(X(t + \Delta t) - X(t)\right)\Big/\left(\Delta t\, X(t)\right) + F(t)/V(t) \tag{8}$$

$$\sigma(t) = \left(F(t)/V(t)\right)\left((S_F - S(t))/X(t)\right) - \left(S(t + \Delta t) - S(t)\right)\Big/\left(\Delta t\, X(t)\right) \tag{9}$$

$$\pi(t) = \left(\left((P(t + \Delta t) - P(t)\right)\Big/\left(\Delta t\, X(t)\right)\right) - \left(F(t)/V(t)\right)\left(P(t)/X(t)\right) \tag{10}$$

where Δt is the time interval between two sampling times.

After the functional expansion of the network inputs is performed, the orthogonal least squares estimator is used to calculate the network weights (w_{ij}) and eliminate nonsignificant nodes *(11)*.

Optimization Problem

Once the process model is determined, Pontryagin's maximum principle *(14)* and the singular control theory are used to solve the optimization problem.

The first step for the solution of this problem is the choice of the control variable. In the literature, the control variable usually chosen is the volumetric feed rate. Alves *(15)*, however, showed that the dilution rate is a more suitable choice. If written as a function of this variable, the mass balance equations for biomass, substrate, and ethanol (Eqs. 1–3) are not explicit functions of the volume of the reactor. Thus, although the global balance equation, Eq. 4, is used to calculate the volume of the reactor, it is not used in the solution of the optimization problem. The dimension of the system is reduced in one order and processes described by four or less mass balance equations can be solved analytically.

Eqs. 1–3, written in a vectorial form, are

$$dx/dt = f(x) + g(x)u \tag{11}$$

with

$$x = \begin{bmatrix} X \\ S \\ P \end{bmatrix}; f(x) = \begin{bmatrix} \mu X \\ -\sigma X \\ \pi X \end{bmatrix}; g(x) = \begin{bmatrix} -X \\ S_F - S \\ -P \end{bmatrix} \text{ and } u = D$$

The following constraints are imposed on the dilution rate and the final (t_f) fermenter volume

$$0 \leq D \leq F_{max}/V(t) \tag{12}$$

$$V(t_f) = V_{max} \tag{13}$$

The optimization problem consists of finding the optimal temporal profile of the dilution rate that leads the reactor from a given initial state to the final state that maximizes the performance index given below:

$$J = P(t_f) \tag{14}$$

This problem can be solved by using Pontryagin's maximum principle. According to this principle, the optimal solution must maximize the Hamiltonian, which is defined as

$$H = \lambda^T(f(x) + g(x)u) \tag{15}$$

where $\lambda(t)$ is the adjoint vector which satisfies

$$d\lambda/dt = -\partial H/\partial x \tag{16}$$

The Hamiltonian can be rewritten as

$$H = \phi(t)u + H_0(t) \tag{17}$$

where

$$\phi(t) = \lambda^T g(x) \tag{18}$$

$$H_0(t) = \lambda^T f(x) \tag{19}$$

Since the Hamiltonian is linear in the control variable, it is easy to determine u(t) which maximizes this Hamiltonian by examining the sign of the function $\phi(t)$.

$$\text{if } \phi(t) > 0 \qquad u = u_{max} \tag{20}$$

$$\text{if } \phi(t) < 0 \qquad u = u_{min} \tag{21}$$

However, if $\phi(t)$ is equal to zero over a finite time interval (t_1, t_2), Pontryagin's maximum principle fails to give u(t) during this interval and

the singular control theory has to be used. This is called the singular interval.

The optimal temporal profile of the control variable has singular ($u = u_{sing}$) and nonsingular ($u = u_{min}$ or $u = u_{max}$) intervals. The complete solution of the optimization problem consists of the determination of the singular dilution rate expression, the switching times between the different values of this variable, and the sequence in which these values appear.

Singular Dilution Rate

During the singular interval, $\phi(t)$ is equal to zero, and hence its derivatives must also vanish. According to the singular control theory, the expression of the control variable in the singular interval can be determined by deriving $\phi(t)$ until the control variable appears explicitly. In the cases studied in this article, the singular dilution rate is determined by making the second derivative of $\phi(t)$ equal to zero.

The following equations can be written in the singular interval:

$$\phi = 0 \tag{22}$$

$$d\phi/dt = 0 \tag{23}$$

$$d^2\phi/dt^2 = 0 \tag{24}$$

In addition, if the fermentation time (t_f) is not specified a priori, the Hamiltonian on the optimal trajectory is equal to zero. Then, during the singular interval,

$$H_0(t) = 0 \tag{25}$$

In this work, Lie brackets *(16)* are used to obtain the singular arc and the singular dilution rate expressions. By using this differential geometric tool, the first derivative of ϕ can be written as

$$d\phi(t)/dt = \lambda^T[f,g](x) \tag{26}$$

where [f,g] is the Lie bracket, which is a vector field defined by

$$[f,g](x) = \left(\partial g(x)/\partial x\right) f(x) - \left(\partial f(x)/\partial x\right) g(x) \tag{27}$$

Its components are given by

$$([f,g](x))_i = \sum_{j=1}^{n} \left(f_j \left(\partial g_i / \partial x_j\right) - g_j \left(\partial f_i / \partial x_j\right)\right) \tag{28}$$

The second derivative of $\phi(t)$ can be written as

$$d^2\phi/dt^2 = \lambda^T[f,[f,g]] + \lambda^T[g,[f,g]]u = \lambda^T ad_f^2 g(x) + \lambda^T ad_g^2 f(x) \quad (29)$$

where $ad_f^2 g(x)$ and $ad_g^2 f(x)$ are the notations used for the iterated Lie brackets [f,[f,g]] and [g,[f,g], respectively.

The singular control is then given by

$$u_s = -\lambda^T ad_f^2 g(x) / \left(\lambda^T ad_g^2 f(x)\right) \quad (30)$$

For systems described by four mass balance equations, because the global balance equation is not used, the effective state variables vector, and thus the adjoint variables vector, are three-dimensional (the volume is not used as a state variable). In this case, it is possible to write two adjoint variables as a function of the third one and of the state variables. From Eq. 22 one can write

$$\lambda_1 = A(x)\lambda_3 \quad (31)$$

And from Eq. 25

$$\lambda_2 = B(x)\lambda_3 \quad (32)$$

The substitution of Eqs. 31 and 32 into Eq. 26 leads to

$$d\phi/dt = \lambda_3 G(x) \quad (33)$$

Then, from Eq. 23, it follows that, in the singular interval

$$G(x) = 0 \quad (34)$$

Also, substituting Eqs. 31 and 32 into Eq. 29, the following equation is obtained:

$$d^2\phi/dt^2 = \lambda_3(a(x) - b(x)u) \quad (35)$$

From Eq. 24 it follows that, in the singular interval

$$u_s = a(x)/b(x) \quad (36)$$

which is the equation of the control variable acting during this interval as a function only of the state variables.

In Eqs. 31–36, A(x), B(x), G(x), a(x), and b(x) are functions of the state variables.

Switching Times

In the literature, the fermentation process studied in this work is considered to present two switching times: The time at which the singular arc is reached (Eq. 34 is valid), and the time at which the maximum volume of the reactor is attained *(17)*.

In this work, the final time of the fermentation is free, and, in this case, at the end of the fermentation the Hamiltonian must be equal to zero. Because at this stage, the reactor is operated in batch mode, the final time is determined from the following equation:

$$H_0(t_f) = 0 \tag{37}$$

Also, because in the problem studied, the terminal point is not fixed a priori, the final value of the adjoint variables is given by

$$\lambda_i(tf) = \left(\partial J / \partial x_i\right)\Big|_{tf} \tag{38}$$

The substitution of Eq. 38 in Eq. 37 enables the determination of the final time of the fermentation.

Control Variable Values Sequence

The sequence in which the values of the control variable appear is determined by the initial conditions. If at the beginning of the fermentation $\phi(0) < 0$, the sequence is ($u = 0$; $u = u_{sing}$; $u = 0$); if $\phi(0) > 0$, it is ($u = u_{max}$; $u = u_{sing}$; $u = 0$) and if $\phi(0) = 0$, the sequence is ($u = u_{sing}$; $u = 0$).

At this point, the optimal temporal profile of the control variable is completely determined. Initially, the dilution rate assumes the maximum or minimum value (depending on the initial conditions) until Eq. 34 is valid. Then, the fermenter is fed with the singular dilution rate until it is full, and after this point it is operated in batch mode until the final condition, given by Eq. 37, is attained.

Adaptive Optimal Control

Once the optimization problem has been solved, the optimal temporal profile is known in terms of the state variables. Actually, the dilution rate expression is a function of the state variables, the specific kinetic rates, and their derivatives, which are functions of the state variables. Then, the following expression can be written:

$$D = D(X, S, P, \mu, \sigma, \pi, \text{derivatives of } \mu, \sigma, \pi) \tag{39}$$

To implement adaptive optimal control, this expression must be recalculated and the kinetic parameters re-estimated at each sampling time. If

experimental measures of the concentrations of biomass, substrate, and ethanol are available, Eqs. 8–10 can be used to determine the specific rates of growth, substrate consumption, and ethanol formation, and these values used to re-estimate the network parameters at each sampling time. Because the network is linear in the parameters, the re-estimation is easy and rapid. As for the kinetic rate derivatives, in this work they are approximated by the derivatives of the corresponding neural networks, with very good results.

RESULTS

Ethanol Production by *S. cerevisae*

This process has been studied by Aiba et al. *(18)* and Modak and Lim *(17)*. The proposed kinetic model is given below:

$$\mu = \left(0.408S/(0.22 + S)\right) \exp(-0.028P) \tag{40}$$

$$\sigma = \mu/0.1 \tag{41}$$

$$\pi = \left(S/0.44 + S)\right) \exp(-0.015P) \tag{42}$$

In this work, this model is used to generate data for the modified FLN training.

Modified Functional Link Network

A neural network will be trained to estimate the specific growth rate:

$$y = [\mu] \tag{43}$$

using the following input

$$x_e = [X\ S\ P]^T \tag{44}$$

Training is based on sets of values of the specific growth rate and biomass, substrate, and ethanol concentrations at different sampling times.

The nonlinear functions $h_j(x_e)$ are obtained through a functional expansion of the inputs in the form of a polynomial expansion of degree six.

The activation function used was

$$f(y) = 1/y \tag{45}$$

After the elimination of monomials with negligible effect, the resulting neural network expression is

$$\mu_{FLN} = 1/\left(2.40 + 0.69/S + 0.082P + 0.00057\ P^2/S + 0.000030P^3\right) \tag{46}$$

The neural network performance was measured by a coefficient denoted by "cor" and defined as follows *(19)*:

$$cor = (1 - SEE/S_{TT})100\% \quad (47)$$

where $SEE = \sum_{k=1}^{N}(y_e(k) - y(k))^2$, $S_{TT} = \sum_{k=1}^{N}(y_e(k) - \overline{y_e})^2$, $y_e(k)$ is the k experimental output, y(k) is the corresponding network output, $\overline{y_e}$ is the mean value of the experimental outputs, and N is the number of experimental data.

The FLN described the experimental data with a correlation of 99.97%.

Optimization Problem

The results of the optimization problem for the conditions: X(0) = 0.2 g/L, S(0) = 100 g/L, P(0) = 0 g/L and V(0) = 5 L, S_F = 100 g/L and V_{max} = 20 L, are shown in Figs. 2 and 3. In Fig. 2, the temporal profiles of the dilution rate calculated using the kinetic model of Aiba et al. *(18)* and the FLN to describe the specific growth rate are shown. Figure 3 shows the temporal profiles of ethanol concentration.

Initially, as $\phi < 0$, the fermenter is operated with the minimum dilution rate (D = 0) until Eq. 34 is valid. At this point, the dilution rate assumes its singular value until the reactor is full. Then, the reactor is operated in batch mode until the final condition is attained, in this case, substrate concentration equal to zero.

In Figs. 2 and 3, it can be seen that the result obtained using the modified neural network to estimate the specific growth rate is similar to the one obtained when this kinetic rate is expressed by the model equation. These results show that the derivative of the neural network can be used to describe the derivative of the model.

Adaptive Optimal Control

To show the applicability of the proposed adaptive optimal control strategy, its results are compared to the results of the open-loop implementation of the precalculated temporal profile in situations in which there is a plant–model mismatch.

Case 1

In this case, it is considered that the ethanol inhibits the specific growth rate less than the model used to calculate the optimal dilution rate profile predicts. In other words, the neural network was trained based on Eq. 40, an imperfect model, but the equation that really describes the specific growth rate is

$$\mu = \left(0.408S/(0.22 + S)\right) \exp(-0.02P) \quad (48)$$

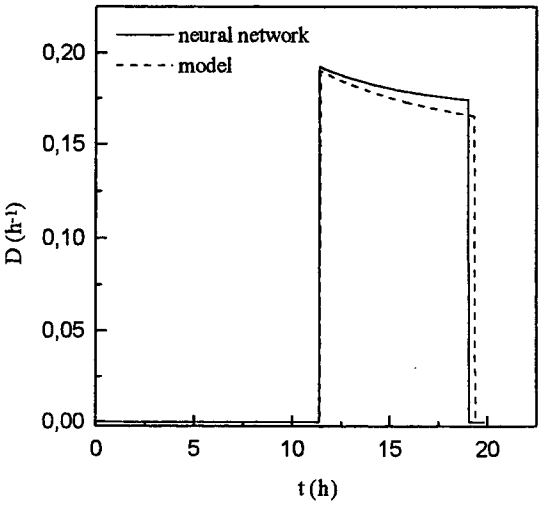

Fig. 2. Temporal profiles of the dilution rate obtained using Aiba et al. *(18)* kinetic model and the FLN to describe the specific growth rate.

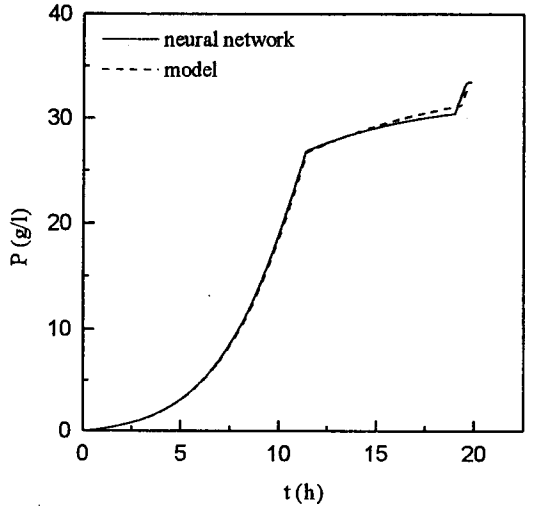

Fig. 3. Temporal profiles of ethanol concentration obtained using Aiba et al. *(18)* kinetic model and the FLN to describe the specific growth rate.

The results of the implementation of the open-loop, the adaptive control, and that which would be obtained if the perfect model (Eq. 48) were used to solve the optimization problem are shown in the Figs. 4 and 5. Figure 4 shows the results in terms of the volumetric substrate feed rate, which is easily calculated from the dilution rate (F = D/V).

Because the real inhibition of the specific growth rate by the ethanol is lower than calculated by the imperfect model, the real substrate con-

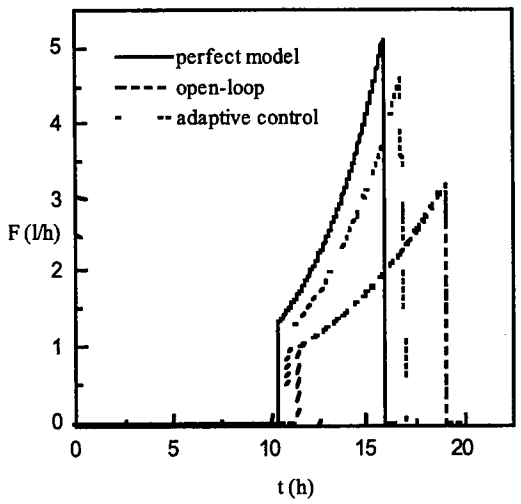

Fig. 4. Temporal profiles of the volumetric substrate feed rate for perfect model, open-loop implementation of the profile based on the imperfect model, and adaptive optimal control. Case 1.

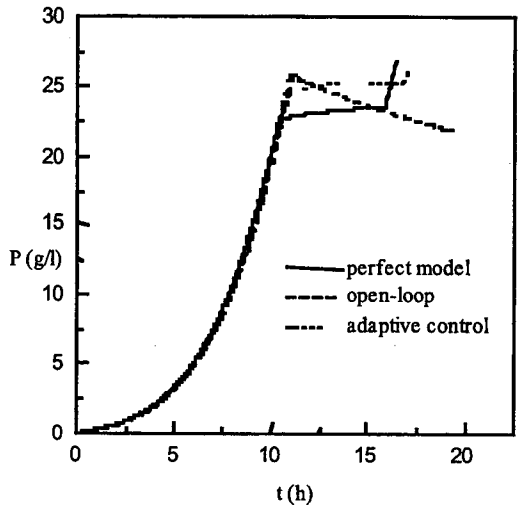

Fig. 5. Temporal profiles of ethanol concentration for perfect model, open-loop implementation of the profile based on the imperfect model, and adaptive optimal control. Case 1.

sumption will be higher than this model predicts. In Fig. 4, it can be seen that the volumetric substrate feed rate calculated using the perfect model is the highest. When the profile calculated based on the imperfect model is implemented in an open-loop fashion, the resulting feed rate is much lower than necessary to obtain the optimal final ethanol concentration. However, when this profile is implemented in the adaptive optimal control

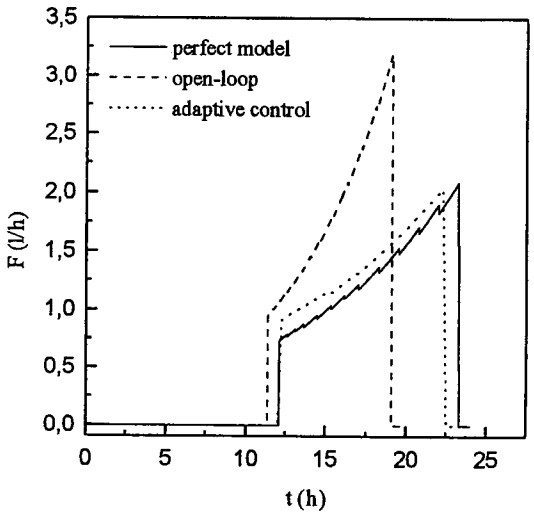

Fig. 6. Temporal profiles of the volumetric substrate feed rate for perfect model, open-loop implementation of the profile based on the imperfect model, and adaptive optimal control. Case 2.

scheme, the resulting dilution rate is similar to the optimal because of the re-estimation of the network parameters.

Figure 5 shows that the result obtained with the adaptive optimal "control scheme is the nearest to the optimal result, obtained by the use of the perfect model. The results obtained with the open-loop implementation, the adaptive optimal scheme, and the perfect model are 22 g/L, 26 g/L, and 26.6 g/L, respectively.

Case 2

In this case it was considered that the ethanol inhibits the specific growth rate more than the model used to calculate the optimal dilution rate profile predicts. The neural network was trained based on Eq. 40, an imperfect model, but the equation which really describes the specific growth rate is given below:

$$\mu = \left(0.408S/(0.22 + S)\right) \exp(-0.033P) \tag{49}$$

In this case, the real substrate consumption is lower that the calculated by the model, and then the dilution rate, or the volumetric substrate feed rate, calculated based on the imperfect model, is higher than that required to obtain the optimal final ethanol concentration. In Figs. 6 and 7, it can be seen that the profiles obtained by the adaptive optimal control are very similar to that obtained by the perfect model. The results of the open-loop implementation, the adaptive optimal scheme, and the perfect model are 32 g/L, 41.4 g/L, and 41.9 g/L, respectively.

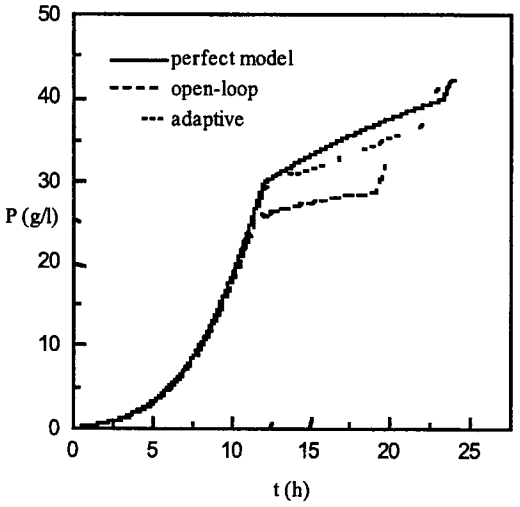

Fig. 7. Temporal profiles of ethanol concentration for perfect model, open-loop implementation of the profile based on the imperfect model, and adaptive optimal control. Case 2.

DISCUSSION

In most cases, the models used to determine the optimal feed policy for fed-batch biochemical processes are developed based on steady state data and work only qualitatively under transient conditions. Besides, strain modification caused by microbial adaptation or a change in the quality of nutrient medium can cause large variations in the values of parameters used to model a system *(20)*. Thus, the development of an adaptive scheme to the optimization of these systems is of extreme importance.

In this work, an adaptive control scheme was developed for the optimization of an ethanol fermentation process. It was based on the development of a hybrid neural model for the process to be optimized. The model, composed by the mass balance equations of the process and modified FLNs, which described the kinetic rates, was shown to reproduce the process dynamics accurately.

The use of the FLNs enabled the re-estimation of the network parameters at each sampling time without much computational effort, because, in these networks, the parameter estimation is linear.

The results of the open-loop implementation when there is a plant–model mismatch showed that the final concentration of ethanol attained in the cases studied was very far from the optimal. However, the adaptive optimal control scheme led to better results.

ACKNOWLEDGMENT

The authors acknowledge CNPq for financial support.

REFERENCES

1. Palanki, S., Kravaris, C., and Wang, H. Y. (1994), *Chem. Eng. Sci.* **49,** 85–97.
2. Cuthrell, J. E. and Biegler, L. T. (1989), *Comput. Chem. Eng.* **13,** 49–62.
3. Luus, R. (1993), *Ind. Eng. Chem. Res.* **32,** 859–865.
4. Costa, A. C.(1996), M.Sc. Thesis, Federal University of Rio de Janeiro, Rio de Janeiro, Brazil.
5. Terwiesch, P. and Agarwal, M. (1994), *Comput. Chem. Eng.* **18,** S433–S437.
6. Lee, J. and Ramirez, W. F. (1996), *Chem. Eng. Sci.* **51,** 521–534.
7. Psichogios, D. C. and Ungar, L. H. (1992), *AICHE J.* **38,** 1499–1511.
8. Schubert, J., Simutis, R., Dors, M., Havlik, I., and Lübbert, A. (1994), *J. Biotechnol.* **35,** 51–68.
9. Fu, P. and Barford, J. P. (1994), *Proceedings of PSE* '94, 571–574.
10. Chen, S. and Billings, S. A. (1992), *Int. J. Control* **56,** 319–346.
11. Henrique, H. M. (1997), Personal communication, COPPE/UFRJ.
12. Billings, S. A., Chen, S., and Koremberg, M. J. (1989), *Int. J. Control* **49,** 2157–2189.
13. Veeramallu, U. and Agrawal, P. (1990), *Biotechnol. Bioeng.* **36,** 694–704.
14. Pontryagin, L. S., Boltyanskii, G. R. V., and Mischenko, E. F. (1962), *Mathematical Theory of Optimal Processes,* Wiley-Interscience, New York.
15. Alves, T. L. M. (1993), DSc. thesis, Federal University of Rio de Janeiro, Rio de Janeiro, Brazil.
16. Kravaris, C. and Kantor, J. C. (1990), *Ind. Eng. Chem. Res.* **29,** 2295–2310.
17. Modak, J. M. and Lim, H. C. (1987), *Biotechnol. Bioeng.* **30,** 528–540.
18. Aiba, S., Shoda, N., and Nagatani, N. (1968), *Biotechnol. Bioeng.* **10,** 845–853.
19. Milton, J. S. and Arnold, J. C. (1990), *Introduction to Probability and Statistics,* McGraw Hill, New York.
20. Agrawal, P., Koshy, G., and Ramseier, M. (1989), *Biotechnol. Bioeng.* **33,** 115–125.